Liquid Crystals
Publication details, including instructions for authors and subscription information:
http://www.informaworld.com/smpp/title~content=t713926090

Preliminary communication Nematic-substrate repulsion in the nematic-isotropic phase coexistence region

Anjun J. Jin; Yi-Kuo Yu; Philip L. Taylor; Charles Rosenblatt

Online publication date: 06 August 2010

To cite this Article Jin, Anjun J. , Yu, Yi-Kuo , Taylor, Philip L. and Rosenblatt, Charles(1998) 'Preliminary communication Nematic-substrate repulsion in the nematic-isotropic phase coexistence region', Liquid Crystals, 24: 6, 891 — 894
To link to this Article: DOI: 10.1080/026782998206722
URL: http://dx.doi.org/10.1080/026782998206722

LIQUID CRYSTALS, 1998, VOL. 24, NO. 6, 891–894

Preliminary communication
Nematic–substrate repulsion in the nematic–isotropic phase coexistence region

by ANJUN J. JIN, YI-KUO YU, PHILIP L. TAYLOR,
and CHARLES ROSENBLATT*

Department of Physics, Case Western Reserve University, Cleveland,
Ohio 44106-7079, USA

(*Received 17 November 1997; accepted 5 December 1997*)

Observations of two types of nematic droplet in the nematic–isotropic phase coexistence region are reported. One type contains topological defects and is free to move within a thin, homeotropically treated cell; the other is defect free and appears to be pinned at the substrates. The freely moving droplet represents an apparently new liquid crystal–substrate repulsion, which depends on the director alignments at the substrate and at the surface of the nematic droplet.

Although there is a considerable body of literature on liquid crystalline droplets dispersed in a dissimilar medium [1, 2], there is little devoted to the subject of nematic droplets floating in a phase-separated isotropic background [3, 4]. Systems of this sort are particularly interesting, as the surface tension may be quite small [5] and short range orientational order may develop across the interface [6]. As part of a larger programme on phase separation phenomena in LCs we have made a preliminary study of the interaction of nematic droplets with substrates that are treated for homeotropic and planar alignment, as well as with substrates that are cleaned but otherwise untreated for any particular alignment. We observed two types of nematic droplet, as well as interactions among droplets and with the substrates. The subject of this communication is an apparent repulsion between the homeotropically prepared substrate and one type of nematic droplet.

In order to observe the behaviour of the LC in the biphasic region, we used a polarizing microscope in conjunction with a 6 μm thick LC cell in a temperature-controlled oven, stabilized to ±2 mK. The glass substrates, which were coated with indium tin oxide, were first cleaned in detergent and distilled water, then acetone, and finally rinsed with ethanol. To make homeotropic cells we spin-coated the polyimide PI7511 (Nissan Chemicals) onto the substrates; for planar alignment we spin-coated the polyimide PI2555 (DuPont) and buffed the surfaces unidirectionally. The substrates for the untreated cells were simply cleaned. The substrates were assembled with Mylar spacers and cemented together; the cells were then filled with the liquid crystal mixture M1106 (Merck), which has a very wide nematic temperature range. Just after filling in the nematic phase, streaks and patches of flow-aligned regions were clearly observed. The oven temperature was then increased to 100°C, which is above the LC clearing temperature $T_c \sim 93$°C. Since ordinarily the cells would appear dark between crossed polarizers when the LC is in the isotropic phase, we set the analyser of the microscope at an angle of 70° from the polarizer in order to have a small amount of transmitted light.

Let us now concentrate on the cell treated for homeotropic alignment. When the cell was slowly cooled to approximately 200 mK below the onset of phase separation (at the middle of the biphasic region, which was approximately 400 mK in extent) we observed the formation of two types of droplet in the isotropic-liquid sea environment. These were (1) homeotropically aligned droplets and (2) nearly circular defect droplets of bipolar disclination structure. We believe that the droplets are nucleated respectively at the surface and within the bulk region of the isotropic sea. The point defects are bipolar (figure 1) with vortex charge $s = \pm 1$ disclinations [7]. Over several hours the droplets coarsened: the defect droplets eventually became elongated and the homeotropic droplets became irregular in shape with a characteristic size of several hundred microns. In this communication we shall concentrate only on the early stages of the phase transition process, from approximately 10–60 min after the onset of phase separation.

*Author for correspondence.

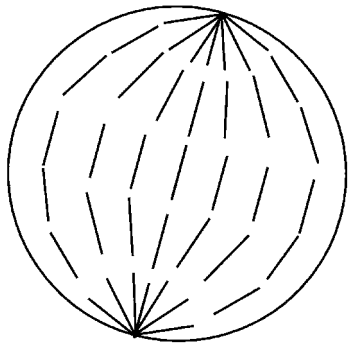

Figure 1. Schematic view of director profile in the defect droplet.

In figure 2 we show sequential video images, from which we see that the homeotropic dark droplets are anchored in position, with their alignment determined by the substrate surface treatment. Furthermore, their size and nearly circular shape are very stable. In contrast, the bipolar defect droplet moves freely across the bulk. These observations hold for all homeotropic and defect droplets in the cell. The free motion of the defect droplet strongly suggests that it is confined to the bulk region in the isotropic sea, *and does not come into contact with the surfaces*. This is our primary observation. We have also observed that when a defect droplet contacts a homeotropic droplet, the defect pattern in the defect droplet tends to rotate. When the bipolar defect region osculates the homeotropic droplet, the droplets begin to merge: homeotropic order propagates into the defect droplet and the defect droplet is absorbed into the overall droplet on time scales of order several seconds. This is illustrated in figures 2(*f*), 2(*g*) and 2(*h*), where the homeotropic droplet (typically tens to 100 μm in diameter) is strongly anchored to the surface. This phenomenon will be the subject of future study.

We also examined both untreated cells and cells treated for planar alignment. In both cases only droplets containing defects were observed; neither uniformly aligned planar droplets nor homeotropic droplets were detected. Moreover, the droplets in these cells were all pinned in position, and the spatial evolution of the disclination cores within the droplets occurred typically over tens of seconds. This is to be compared with the much more rapid (~1 s) times associated with motion of the disclinations in the defect droplets in the homeotropic cell. This indicates that the defects in the planar and untreated cells are controlled by the substrate, whereas the disclination motion in the defect droplet of the homeotropic cell is unimpeded by the substrate. Moreover, this gives further evidence that the defect droplets in the homeotropic cell are not in contact with the substrate. Clearly there is an inherent difference between the defect droplets in the homeotropic cell and those in the planar and untreated cells. From our body of observations we conclude that there is a repulsive interaction between the homeotropically prepared substrate

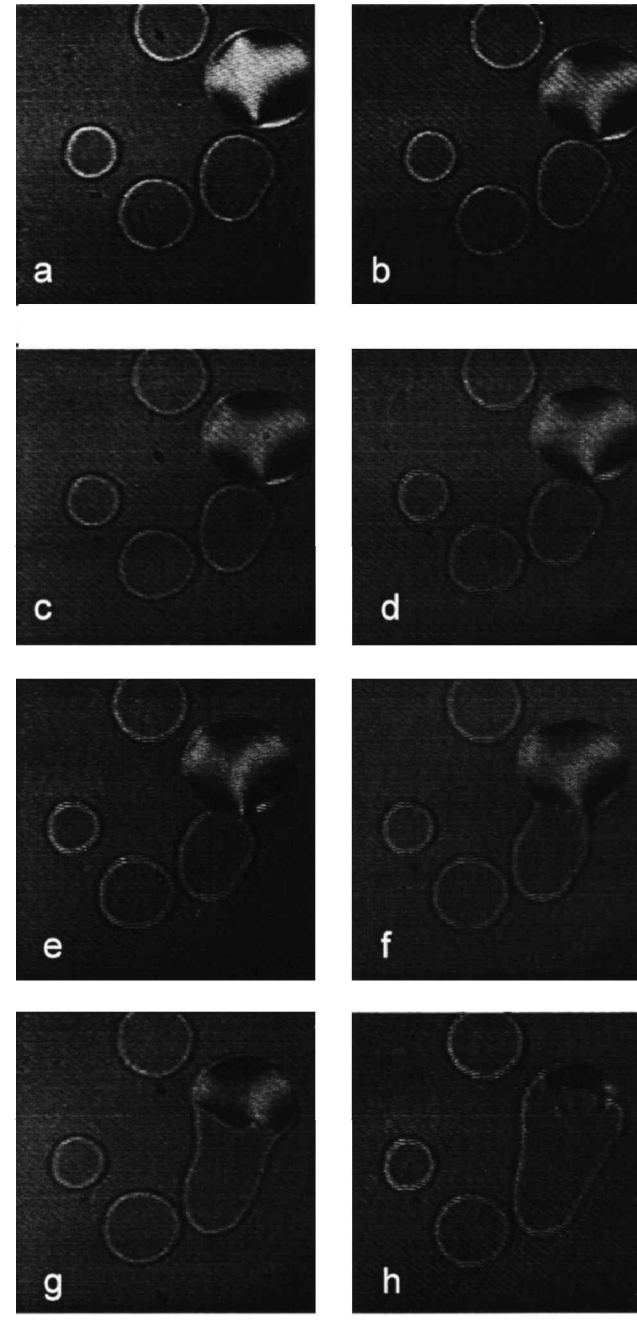

Figure 2. Sequence of images of homeotropic and defect droplets in the homeotropic cell. Images (*a*)–(*e*) are temporally spaced approximately 100 ms, with subsequent images spaced approximately 200 ms. The defect droplet is approximately 100 μm in diameter, it is initially mobile, and eventually merges with the fixed homeotropic droplet; the homeotropic droplets are uniformly dark with a bright outer ring. Subsequently, homeotropic order propagates into the merged droplet.

and the defect droplets which nucleate in the bulk interior of the cell. Additionally, our observations indicate that it is the homeotropic substrate preparation rather than, e.g. chemical composition gradients (which would not distinguish between substrate preparations), that plays the dominant role in this repulsion.

Let us examine why a bipolar nematic defect that has been nucleated in the bulk isotropic sea cannot grow to touch the homeotropically treated substrate. First, when the droplet size is small compared with the cell spacing, bulk elastic forces and the surface energy determine the droplet shape. We can estimate the droplet shape from dimensional arguments. In the limit of strong anchoring [8] the free energy of a spherical droplet of radius ρ is $F_{\text{sphere}} \sim K\rho^{-2}(4\pi\rho^3/3) + 4\pi\rho^2\sigma$, where K is an elastic constant associated primarily with bend and splay distortions [9] and σ is the nematic–isotropic surface tension. If the droplet flattens out into an oblate (pancake) shape of radius a and thickness h, we can take its free energy as $F_{\text{oblate}} \sim (2\pi a^2 + 2\pi ah)\sigma$. For the oblate droplet we assume that the director is oriented uniformly parallel to the plane of the pancake and neglect edge deformations, thereby eliminating the elastic terms. With the constraint of constant droplet volume and estimating $K \sim 5 \times 10^{-7}$ erg cm^{-1} [10] and $\sigma \sim 0{\cdot}15$ erg cm^{-2} [5], we find that for $\rho_{\text{critical}} \gtrsim 0{\cdot}1\,\mu$m the free energy F_{sphere} is always smaller than F_{oblate}. Moreover, for weak anchoring the elastic distortion would be reduced, and ρ_{critical} would be even smaller. Thus small droplets, down to $\sim 0{\cdot}1\,\mu$m, are spherical.

Continuing this line of reasoning, imagine now that the director configuration of the defect droplet is parallel to its surface. When the droplet grows to a size comparable (but not quite equal) to the cell spacing, the incompatibility between the (homeotropic) director orientation at the substrate surface and the planar orientation at the droplet surface creates an elastic energy cost. Further growth of the droplet will therefore be *lateral*, albeit at the expense of an increase in surface energy. This droplet flattening process has an additional advantage. By reducing the curvature of the now flat part of the droplet, the local elastic energy inside the droplet decreases because the director configuration corresponds to that at the droplet's surface.

For a large oblate defect droplet the major portion of its surface is coplanar with the substrate, with a thin region of isotropic phase in between. The director profile of the defect droplet is determined by several competing factors, including the free energies associated with the surface tension and the elastic distortion energy. Near the substrate the molecules are homeotropically aligned by the substrate preparation over a distance approximately ξ into the bulk liquid crystal, where ξ corresponds to the nematic correlation length and is typically of order 100 Å. Away from this region the phase is isotropic. Likewise, the mostly planar order at the surface of the defect droplet can propagate a distance of order ξ into the isotropic phase toward the substrate. Therefore, in order that there be an intermediate region of isotropic phase between the droplet and the substrate, the thickness of this region must be at least 2ξ. Now consider a small, thermally generated, hemispherical bump of radius ξ at the surface of the droplet that just reaches the ordered region a distance ξ from the substrate. In the spirit of our earlier dimensional calculation, the excess free energy due to the nematic–isotropic surface tension is $\delta F_{\sigma 1} \sim \pi\xi^2\sigma$. However, once the top of the bump makes contact with the substrate region there is a reduction of this surface energy. This decrease is associated with the partial disappearance of the domain boundary due to an orientational change from the mostly planar orientation at the droplet to homeotropic orientation at the substrate, *viz.* $\delta F_{\sigma 2} \sim -\frac{1}{2}\Omega\xi^2$. Here $\Omega \sim 1$ steradian is the solid angle within which the homeotropic orientation at the substrate and the orientation at the top of the bump mutually align. Finally, the cost of the elastic distortion associated with the hemispherical bump is $\delta F_{\text{e}} \sim K\xi^{-2}(2\pi\xi^3/3)$. The elastic term comes about from a director distribution in the bump (figure 3) which is similar to, but not quite the same as, an 'escaped radial' configuration [1, 2]. The total incremental free energy is $\delta F_{\text{tot}} \sim \xi[2\pi K/3 + \xi\sigma(\pi - \Omega)]$. Again taking $K \sim 5 \times 10^{-7}$ dyn, $\sigma \sim 0{\cdot}15$ erg cm^{-2} and $\xi = 10^{-6}$ cm, we find $\delta F_{\text{tot}} \sim 10^{-12}$ erg [$\gg k_{\text{B}}T$]. The defect droplet therefore remains stable in the bulk as a thermally generated bump entails a large energy cost. However, as δF_{tot} is about an order of magnitude larger than $k_{\text{B}}T$, the stability of the defect droplet may be affected by variations of these parameters with temperature and material. For example, for sufficiently small ξ or K, the defect droplets may merge with the substrate: at slightly lower temperatures in the biphasic region and for sufficiently long times, an occasional defect droplet was

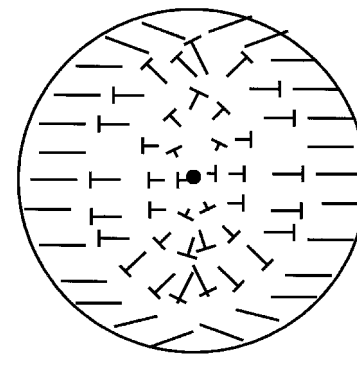

Figure 3. Schematic representation of the top view of the director profile in a hemispherical bump.

observed to spontaneously become a pinned homeotropic droplet. We note that although we believe this pinning process was due to thermal generation of bumps, other processes may also be at play. For example, local defects in the homeotropic order at the cell's surface could have given rise to a local director profile which easily matched the surface director profile of the droplet, thereby pinning the droplet. That spontaneous pinning and conversion to homeotropic orientation seems to be temperature dependent and requires very long times (tens of minutes) argues—although not conclusively—for the thermally generated bump mechanism. Both mechanisms, of course, may operate simultaneously.

It is important to note that our simple model compares the energies associated only with the initial and final configurations. In general there will be an energy barrier between these states due to, for example, orientational anchoring at the droplet and substrate surfaces. This barrier, which is always larger than the initial–final energy separation, will further hinder the approach of the droplet to the substrate, even if δF_{tot} is comparable to $k_{\mathrm{B}}T$. Additionally, note that bumps smaller than the nematic correlation length ξ are not feasible.

Although it is unlikely that a thermally generated bump could facilitate the merger of the defect droplet with the homeotropic substrate, another possible mechanism for a merger is by uniform translation along an axis normal to the cell. We note, however, that if the droplet attempts to approach within 2ξ of the substrate, there would be an appreciable elastic energy cost arising from the mismatched director orientations at the droplet and substrate surfaces. Thus, merger is prevented. This mechanism is similar to that which prevents droplets from growing laterally upon nucleation in the cell's interior. We therefore conclude that the defect droplet in the homeotropic cell is repelled by the substrate, and the defect droplet is free to move laterally within the cell.

In summary, we have classified a new type of interaction, i.e. a repulsion between a nematic droplet in the nematic–isotropic phase coexistence region and a homeotropically treated substrate. We have speculated about the origin of the repulsion, and offered a simple model based on a tradeoff between elastic and surface energy terms.

The authors wish to thank Jonathan Stott for fruitful discussions. This work was supported by the NSF Advanced Liquid Crystalline Optical Materials Science and Technology Center (ALCOM) under grant DMR-8920147.

References

[1] Drzaic, P. S., 1994, *Liquid Crystal Dispersions* (Singapore: World Scientific).
[2] Crawford, G. P., and Zumer, S., 1996, in *Liquid Crystals and Complex Fluids*, edited by G. P. Crawford and S. Zumer (London: Taylor and Francis).
[3] Park, C. S., Clark, N. A., and Noble, R. D., 1994, *Phys. Rev. Lett.*, **72,** 1838.
[4] Meyer, R. B., 1969, *Phys. Rev. Lett.*, **22,** 918.
[5] Smith, G. W., Vaz, N. A., and Vansteenkiste, T. H., 1989, *Mol. Cryst. liq. Cryst.*, **174,** 49.
[6] Jérôme, B., 1991, *Rep. Prog. Phys.*, **54,** 391.
[7] Crawford, G. P., Doane, J. W., and Zumer, S., 1997, in *Handbook of Liquid Crystal Research*, edited by J. S. Patel and P. J. Collings (Oxford: Oxford University Press).
[8] Blinov, L. M., Kabayenkov, A. Yu., and Sonin, A. A., 1989, *Liq. Cryst.*, **5,** 645.
[9] Jin, A. J., Yu, Y.-K., Taylor, P. L., and Rosenblatt, C. (to be published).
[10] Chandrasekhar, S., 1992, *Liquid Crystals* (Cambridge: Cambridge University Press).